Biointerface Research in Applied Chemistry
Open-Access Journal (ISSN: 2069-5837)

Article
Volume 16, Issue 3, 2026, 91
https://doi.org/10.33263/BRIAC163.091

4-Benzyl-1,3-oxazolidin-2-one as a Multi-target Neuroprotective Candidate Against Parkinson's Disease: An Integrative In Silico Study of Pharmacokinetics, Molecular Docking and Normal Mode Analysis

Anish Singh [1], Diksha Dalal [2], Lovedeep Singh [1,*]

[1] University Institute of Pharma Sciences, Chandigarh University, Mohali, Punjab, India; anish.r262@cumail.in (A.S.); lovedeep.e13279@cumail.in (L.S.);
[2] School of Pharmaceutical Sciences, CGC University, Mohali, Punjab, India; diksha.j4121@cgcuniversity.in;
* Correspondence:lovedeep.e13279@cumail.in;

Received: 11.12.2025; Accepted: 15.05.2026; Published: 15.05.2026

Abstract: Parkinson's disease (PD) is a progressive neurodegenerative disorder characterized by dopaminergic neuronal loss, oxidative stress, protein aggregation, and chronic neuroinflammation. Owing to the multifactorial nature of PD, multi-target small molecules with favorable pharmacokinetic and neuroprotective profiles are increasingly explored as therapeutic candidates. The present study evaluates the pharmacokinetic, toxicological, molecular docking, and molecular simulation properties of the 4-Benzyl-1,3-oxazolidin-2-one heterocyclic scaffold, with potential neuroprotective relevance. ADMET predictions (pkCSM, SwissADME) revealed excellent gastrointestinal absorption, blood-brain barrier (BBB) permeability, moderate plasma protein binding, and a predictable metabolic profile, with overall non-carcinogenic and non-cardiotoxic toxicity parameters. In molecular docking analysis, 4-Benzyl-1,3-oxazolidin-2-one demonstrated moderate binding affinity toward NF-κB (-5.5 kcal/mol), TNF-α (-6.2 kcal/mol), α-synuclein (-5.1 kcal/mol), and the dopamine receptor (-7.6 kcal/mol). However, its docking scores were comparatively lower than those of standard ligands, including parthenolide, adalimumab, anle-138B, and bromocriptine, suggesting relatively weak binding interactions across the selected targets and potential multi-target modulatory activity. Normal Mode Analysis, B-factor evaluation, RMSF, eigenvalue profiling, and covariance mapping revealed distinct binding dynamics, with the compound stabilizing dopamine-associated protein environments more strongly than intrinsically disordered α-synuclein. Collectively, these integrated computational findings suggest that 4-Benzyl-1,3-oxazolidin-2-one exhibits promising pharmacokinetic, anti-inflammatory, and anti-aggregation attributes, supporting its candidacy as a multi-target therapeutic lead for further investigation in PD.

Keywords: 4-benzyl-1,3-oxazolidin-2-one; Parkinson's disease; docking; molecular simulations.

1. Introduction

PD is the second most common neurodegenerative disorder worldwide and continues to increase in prevalence, contributing significantly to global disability and socioeconomic burden [1, 2]. Clinically, PD presents with cardinal motor impairments, bradykinesia, rigidity, resting tremor, and postural instability, along with a diverse range of non-motor symptoms

such as cognitive decline, sleep disturbances, depression, autonomic dysfunction, and hyposmia [3, 4]. These manifestations reflect the multisystemic pathology of PD, including dopaminergic neuronal degeneration in the substantia nigra pars compacta, striatal dopamine depletion, and widespread synaptic impairment [5, 6]. At the molecular level, PD is strongly associated with α-synuclein misfolding and aggregation, leading to the formation of Lewy bodies and Lewy neurites, which disrupt proteostasis, mitochondrial function, and autophagy [7, 8]. Parallel to these events, chronic microglial activation amplifies neuroinflammation through cytokines such as tumor necrosis factor-alpha (TNF-α), interleukin-1 beta (IL-1β), and interleukin-6 (IL-6), which further accelerate neurodegeneration [9, 10]. Mitochondrial dysfunction, characterized by compromised electron transport chain activity and increased reactive oxygen species generation, remains a major driver of neuronal vulnerability in PD [11, 12]. Despite advances in understanding PD mechanisms, current therapies, including levodopa, dopamine agonists, and monoamine oxidase B (MAO-B) inhibitors, provide only symptomatic benefits without modifying disease progression [13, 1]. Consequently, there is growing interest in multi-target small molecules capable of simultaneously modulating α-synuclein aggregation, oxidative stress, neuroinflammation, and mitochondrial impairment [14]. These targets were selected to represent interconnected pathways involved in PD pathogenesis, specifically linking neuroinflammation and protein aggregation. Nuclear Factor kappa-light-chain-enhancer of activated B cells (NF-κB) acts as a central transcriptional regulator of pro-inflammatory cytokines, including TNF-α and IL-6, while α-synuclein aggregation further amplifies inflammatory signaling through microglial activation. Heterocyclic scaffolds remain central to modern central nervous system (CNS) drug discovery due to their structural adaptability, pharmacokinetic suitability, and high potential for BBB permeability [4, 9]. Among these scaffolds, oxazolidinone derivatives exhibit antimicrobial, antioxidant, anti-inflammatory, and emerging neuroprotective properties, positioning them as promising candidates for neurodegenerative disease drug development [14]. 4-Benzyl-1,3-oxazolidin-2-one is structurally favorable for CNS penetration, yet its neuroprotective potential in PD remains uncharacterized. Computational drug discovery, encompassing ADMET prediction, molecular docking, and normal mode analysis, provides a high-efficiency strategy for early-stage profiling of novel CNS-active compounds [15, 16]. These approaches allow accurate prediction of pharmacokinetics, toxicity, binding affinity, conformational dynamics, and protein-ligand stability [5, 6]. Given the multifactorial pathogenesis of PD and the interconnected roles of inflammatory and protein aggregation pathways, we hypothesize that 4-Benzyl-1,3-oxazolidin-2-one may exhibit multitarget neuroprotective potential by modulating NF-κB-mediated inflammatory signaling and α-synuclein-associated pathogenic mechanisms. To explore this hypothesis, we investigate ADMET properties, toxicity profile, docking interactions, and MD-based structural stability of 4-Benzyl-1,3-oxazolidin-2-one against key PD targets, including NF-κB, TNF-α, the dopamine receptor complex, and α-synuclein. Through integrated computational insights, this work aims to evaluate the therapeutic potential of 4-Benzyl-1,3-oxazolidin-2-one as a multi-target neuroprotective candidate for PD.

2. Materials and Methods

2.1. Pharmacokinetics and toxicity.

Pharmacokinetic and toxicity properties were predicted using two independent in silico platforms: SwissADME (Swiss Institute of Bioinformatics) and pkCSM [17]. The canonical SMILES format of 4-Benzyl-1,3-oxazolidin-2-one was used as input for both servers. Default prediction models were applied without modification of internal algorithm parameters.

SwissADME was employed to evaluate physicochemical properties, lipophilicity (LogP), water solubility, gastrointestinal (GI) absorption, BBB permeability, drug-likeness (Lipinski, Veber, Ghose, Egan, and Muegge filters), and medicinal chemistry alerts. pkCSM was used to predict absorption, distribution, metabolism (CYP450 interactions), excretion parameters, and toxicity endpoints, including AMES mutagenicity and hepatotoxicity [18, 19]. All predictions were performed using the web-server versions available at the time of analysis (accessed on: [January, 2026]).

2.2. Molecular docking.

An in silico approach to drug design is an excellent technique that involves designing drugs based on predicted interactions between the ligand and the receptor (disease target). To conduct the molecular docking analysis, PyRx software has been utilized. The most stable forms of the compounds were selected with caution, and their analysis was conducted by using version 20.1 of the Discovery Studio 2025 Client software [20].

2.3. Preparation of ligands.

The chemical structure of 4-Benzyl-1,3-oxazolidin-2-one was obtained in SDF format and converted into Protein Data Bank (PDB) format for docking analysis. The ligand geometry was optimized using standard force-field parameters to achieve a stable conformation. Prior to docking, polar hydrogens were added, rotatable bonds were defined, and appropriate partial charges were assigned. The prepared ligand structure was subsequently used for molecular docking under standardized computational settings.

2.4. Protein selection and preparation.

These targets were selected to represent interconnected pathways involved in PD pathogenesis, specifically linking neuroinflammation and protein aggregation. NF-κB acts as a central transcriptional regulator of pro-inflammatory cytokines, including TNF-α and IL-6, while α-synuclein aggregation further amplifies inflammatory signaling through microglial activation. Secondary targets, including the dopamine receptor complex and α-synuclein, are now explicitly described as exploratory or supportive targets rather than equivalent primary endpoints. The three-dimensional structure of α-synuclein was obtained from the (PDB ID: 1XQ8). As α-synuclein is intrinsically disordered under physiological conditions, this entry represents a structured fragment determined under specific experimental conditions rather than the full-length native protein. The receptor/protein structures (PDB IDs: 1XQ8, 6CM4, 1TNF, and 1NFK) can be downloaded as PDB files from the PDB website. Removed the hetero atoms and water molecules of the receptor. The hydrogen was added together with the grid box. The clusters were further discussed in terms of binding energy, ligand efficiency, constant inhibitor, intermolecular energy, van der Waals interactions, electrostatic energies, etc. An interaction

study was conducted on the ligand's binding mode to the most favorable binding-energy conformation in Discovery Studio Illuminate (2025). Molecular docking shows the binding of the ligands and the receptor, and the affinity of the ligands to the receptor.

2.5. Docking protocol and grid parameters.

Molecular docking was performed using the CB-Dock2 platform. The docking grid box was automatically defined based on cavity detection; however, the grid center coordinates and box dimensions for each target are now explicitly reported in Table 1. Exhaustiveness parameters and scoring functions were maintained at default validated settings unless otherwise specified. These parameters are now clearly described to ensure methodological transparency and reproducibility.

2.6. Docking validation.

To validate the docking protocol, the co-crystallized ligand of each target protein was re-docked into its respective binding site using identical parameters. The root-mean-square deviation (RMSD) between the experimental and predicted binding poses was calculated [21]. An RMSD value < 2.0 Å was considered acceptable, confirming the reliability of the docking setup as shown in Table 3. Additionally, known reference inhibitors for each target were docked under identical computational conditions to provide comparative benchmarking of binding affinities and interaction profiles. This comparative approach enabled contextual interpretation of the docking scores obtained for the test compound.

2.7. Ligand-receptor binding interaction with 2D and 3D structures.

Ligand receptor interactions in a molecular docking are computed to understand ligand-receptor binding to predict exactly how a small molecule (ligand) is fitted into the binding domain of a target protein (receptor). It consists of two main elements: the search algorithm to sample possible binding conformations, and the scoring function to approximate the binding strength using inter-atomic energies, such as hydrogen bonding, van der Waals forces, and ruckelraumbeherts interactions, as shown in Table 2 [22].

2.8. Normal mode analysis (NMA).

The NMA studies of the 4-Benzyl-1,3-oxazolidin-2-one-target complexes were performed using the iMODS web server to evaluate the intrinsic motions and stability of the protein-ligand complex through NMA [23]. The Root Mean Square Fluctuation (RMSF) values were further analyzed using the CABS-flex 2.0 server, which provides coarse-grained simulations of protein flexibility under near-native conditions [24]. Additionally, the Radius of Gyration (Rg) was calculated to assess the compactness and conformational stability of the complexes using computational resources provided by the Supercomputer Facility at the Indian Institute of Technology (IIT) Delhi. These combined simulations offered insights into the structural dynamics, conformational changes, and overall stability of the 4-Benzyl-1,3-oxazolidin-2-one-protein interactions.

2.9. Conformational dynamics analysis.

Conformational stability of any selected protein-ligand complex was measured with the help of NMA according to a coarse-grained elastic network model. The reason for selecting this approach was to determine collective motions and intrinsic flexibility in a computationally efficient manner suitable for preliminary stability analysis. In contrast to atomistic molecular dynamics simulations, NMA is not a time-dependent simulation; it approximates harmonic motions about an energy-minimized structure. NMA was deemed appropriate in the early stages of computational screening, and the fact that full-atomistic MD simulations would be more instructive for the dynamical picture in future investigations.

3. Results and Discussion

3.1. Pharmacokinetics and toxicity profile.

3.1.1. PkCSM analysis.

The evaluated heterocyclic compound (MW: 177.20 g/mol, LogP: 1.34) exhibits favorable physicochemical properties, including a low molecular weight, moderate lipophilicity, limited rotatable bonds, and a surface area of 38.33 Å^2, all of which support optimal drug-likeness. The pharmacokinetic predictions indicate good GI absorption, as reflected by acceptable Caco-2 permeability (-4.53 logPaap), high human intestinal absorption, and bioavailability at both 20% and 50% thresholds. The compound is neither a P-glycoprotein inhibitor nor a substrate, further supporting efficient passive absorption. Distribution parameters reveal the ability to permeate the BBB, evidenced by a logPS of -1.78 and a penetrability score of 1.0, along with moderate plasma protein binding (35.24%) and a suitable steady-state volume of distribution (logVDss: 1.4). Metabolic profiling shows mixed interactions with CYP450 enzymes: while it acts as an inhibitor and substrate of CYP1A2 and a substrate for CYP2D6, it does not inhibit major isoenzymes such as CYP2C9, CYP2C19, or CYP3A4, suggesting a predictable metabolic fate. The compound demonstrates moderate clearance (1.55 log mL/min/kg) and a short-predicted half-life (<3 h), indicating rapid systemic elimination. Importantly, the toxicity profile reflects both favorable and cautionary signals. While the compound is predicted to be non-carcinogenic, non-hepatotoxic (DILI-I negative), non-cardiotoxic (hERG safe), and devoid of endocrine, aquatic, or respiratory toxicity alerts, in silico models indicate potential AMES mutagenicity, micronucleus positivity, crustacean toxicity, skin sensitization risk, and poor biodegradability. These findings suggest that although no major organ-specific or life-threatening toxicities are predicted, genotoxicity-related alerts warrant further experimental validation and structural refinement. Additional physicochemical properties-including a melting point of 95.57°C, hydration free energy of -10.34 kcal/mol, and acceptable solubility and ionization constants (pKa acid 6.72; pKa base 7.61)-further confirm the compound's balanced stability and drug-like attributes. Collectively, these data suggest that the molecule exhibits good oral absorption, efficient BBB penetration, and acceptable systemic distribution, although specific toxicity alerts merit consideration for future structural optimization. Instead, it demonstrates an acceptable organ-toxicity profile with a specific genotoxicity alert that warrants experimental validation (e.g., in vitro AMES assay, micronucleus test) and, if necessary, structural optimization.

3.2. SWISS ADME.

The displayed BOILED-Egg diagram provides a graphical estimation of passive GI absorption (HIA) and BBB penetration based on two key molecular descriptors:

WLOGP (lipophilicity) - plotted on the Y-axis

TPSA (topological polar surface area) - plotted on the X-axis

3.2.1. Yellow region (BBB zone).

The yellow ellipse represents the physicochemical space associated with a high probability of BBB penetration. Compounds positioned within this region are predicted to cross the BBB efficiently through passive diffusion.

3.2.2. White region (HIA zone.

The white ellipse indicates the region associated with high human intestinal absorption. Molecules falling within this area are predicted to be well absorbed in the GI tract, as shown in Figure 1.

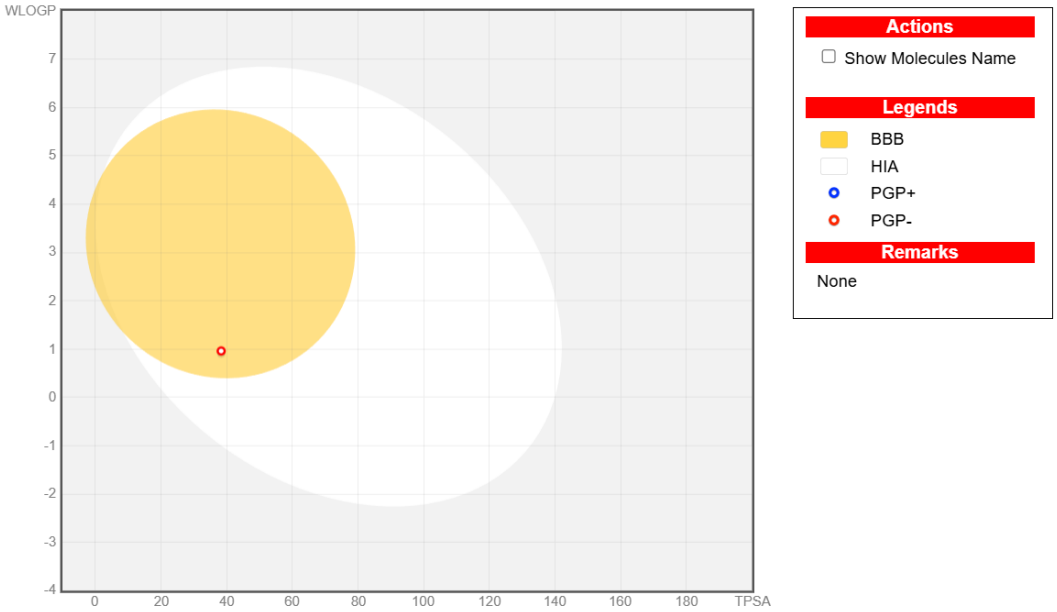

Figure 1. BOILED-Egg structure of 4-Benzyl-1,3-oxazolidin-2-one Via SwissADME.

The BOILED-Egg analysis reveals that the molecule exhibits highly favorable pharmacokinetic properties for CNS targeting. Its position within the yellow region of the plot indicates a strong likelihood of crossing the BBB, an essential requirement for neuroprotective and neurotherapeutic agents. Simultaneously, the molecule also falls within the white HIA zone, suggesting excellent human intestinal absorption and suitability for oral administration. The red-circled marker reflects a P-gp-negative (PGP-) profile, meaning the compound is not a substrate for P-glycoprotein efflux transporters. This feature further enhances its potential for sustained brain availability, as efflux through P-gp commonly limits CNS penetration of many molecules. With an optimal combination of moderate lipophilicity (WLOGP ~1) and low polar surface area (TPSA ~40 Å^2), the molecule demonstrates a physicochemical balance consistent with good permeability and oral bioavailability. Overall, the BOILED-Egg predictive model strongly supports this compound as a promising candidate for CNS-active drug development.

3.3. Molecular docking.

The molecular docking analysis of 4-Benzyl-1,3-oxazolidin-2-one revealed differential binding affinities across key PD-associated targets. Against NF-κB (PDB: 1NFK), the ligand exhibited a docking score of -5.5 kcal/mol, forming hydrogen bonds and hydrophobic contacts within the transcription factor's active pocket, suggesting potential inhibition of pro-inflammatory gene activation. Binding to TNF-α (PDB: 1TNF) showed improved affinity (-6.2 kcal/mol), with stabilizing interactions that may attenuate cytokine-mediated inflammatory signaling. Interaction with α-synuclein (PDB: 1XQ8) demonstrated a score of -5.1 kcal/mol, indicating moderate stabilization within the aggregation-prone region, possibly affecting fibrillation dynamics. The strongest affinity was observed for the dopamine receptor complex (PDB: 6CM4), with a docking score of -7.6 kcal/mol, reflecting multiple stabilizing interactions with dopamine receptors. In the case of NF-κB (PDB: 1NFK), the test compound bonded with an energy of -5.5 kcal/mol, and the reference inhibitor, Parthenolide, bonded with an energy of -6.4 kcal/mol, forming more stable complexes. In the same way, in the case of TNF- against TNF- PDB ID: 1TNF), 4-Benzyl-1,3-oxazolidin-2-one showed a docking score of -6.2 kcal/mol, which is slightly lower than that of the standard adalimumab (-6.7 kcal/mol). In the 3D structure of 1XQ8, the binding energy was found to be -5.1 kcal/mol as compared to -6.4 kcal/mol of Anle-138B, indicating that the compound lacks binding strength with the known aggregation inhibitor, as shown in Table 1. The dopamine receptor (PDB ID: 6CM4) was found to differ most of all with the test compound, as it obtained -7.6 kcal/mol, whereas Bromocryptine, a clinically established dopaminergic agonist, exhibited much stronger interaction (-9.3 kcal/mol). Overall, although the binding energies are slightly lower than those of standard ligands, the compound consistently demonstrates stable, moderate interactions with multiple PD-related targets, supporting its potential as a multi-target lead scaffold, as shown in Figures 2 to 5. Molecular interaction and docking revalidation are now shown in Tables 2 and 3.

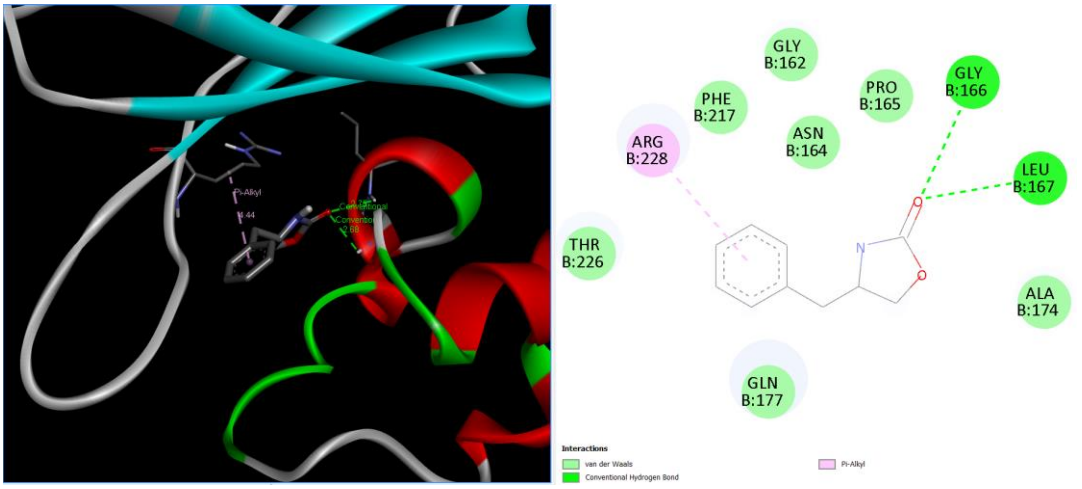

Figure 2. Molecular docking interaction of 4-Benzyl-1,3-oxazolidin-2-one with NF-κB (PDB ID: 1NFK). The ligand exhibits moderate affinity toward NF-κB, reflected by a docking score of -5.5 kcal/mol (Table 1). Interaction mapping reveals hydrogen-bonding and hydrophobic stabilization within the NF-κB binding pocket, suggesting a potential inhibitory influence on transcriptional activation of inflammation-associated genes.

Table 1. Binding energy score of 4-Benzyl-1,3-oxazolidin-2-one and standard drugs with various key targets.

Sr. no	Molecule	PDB ID	Protein name	Grid size	Exhaust i-viness	Binding energy	Ligand efficiency
1.	**4-Benzyl-1,3-oxazolidin-2-one**	**1NFK**	NF-κB	26 × 32 × 32 Å	8	-5.5 Kcal/mol	0.39

Sr. no	Molecule	PDB ID	Protein name	Grid size	Exhaust i-viness	Binding energy	Ligand efficiency
2.	4-Benzyl-1,3-oxazolidin-2-one	1TNF	TNF-α	27 × 20 × 20 Å	8	-6.2 Kcal/mol	0.44
3.	4-Benzyl-1,3-oxazolidin-2-one	1XQ8	α-Synuclein	20 × 26 × 26 Å	8	-5.1 Kcal/mol	0.36
4.	4-Benzyl-1,3-oxazolidin-2-one	6CM4	Dopamine receptor	20 × 20 × 20 Å	8	-7.6 Kcal/mol	0.54
5.	Anle-138B	1XQ8	α-Synuclein	26 × 26 × 26 Å	8	-6.4 Kcal/mol	0.29
6.	Bromocriptine	6CM4	Dopamine receptor	20 × 20 × 20 Å	8	-9.3 Kcal/mol	0.21
7.	Adalimumab	1TNF	TNF-α	20 × 20 × 20 Å	8	-6.7 Kcal/mol	0.32
8.	Parthenolide	1NFK	NF-κB	35 × 35 × 35 Å	8	-6.4 Kcal/mol	0.43

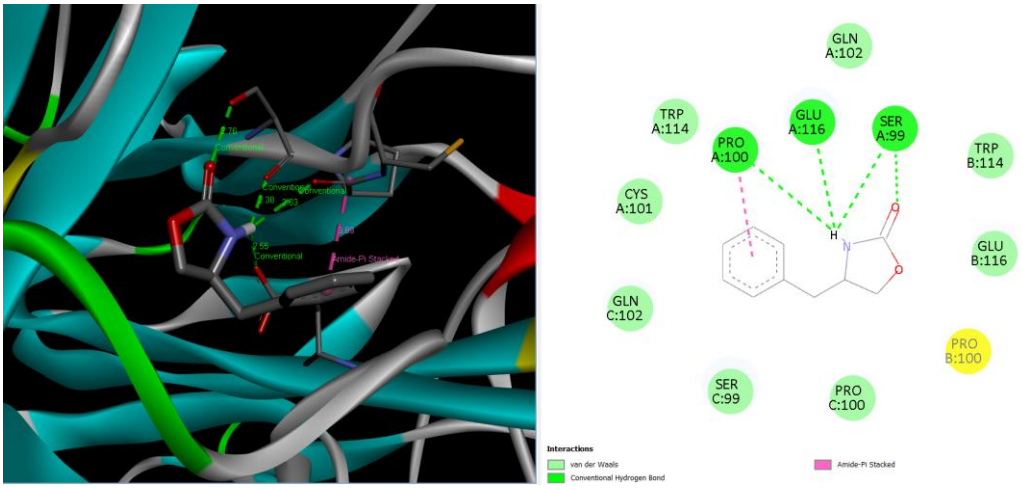

Figure 3. Molecular docking interaction of 4-Benzyl-1,3-oxazolidin-2-one with TNF-α (PDB ID: 1TNF). With a docking score of -6.2 kcal/mol, the ligand displays appreciable binding affinity for TNF-α. The interaction profile highlights key stabilizing contacts that may interfere with TNF-α-mediated signaling, supporting its possible modulatory role in inflammatory responses.

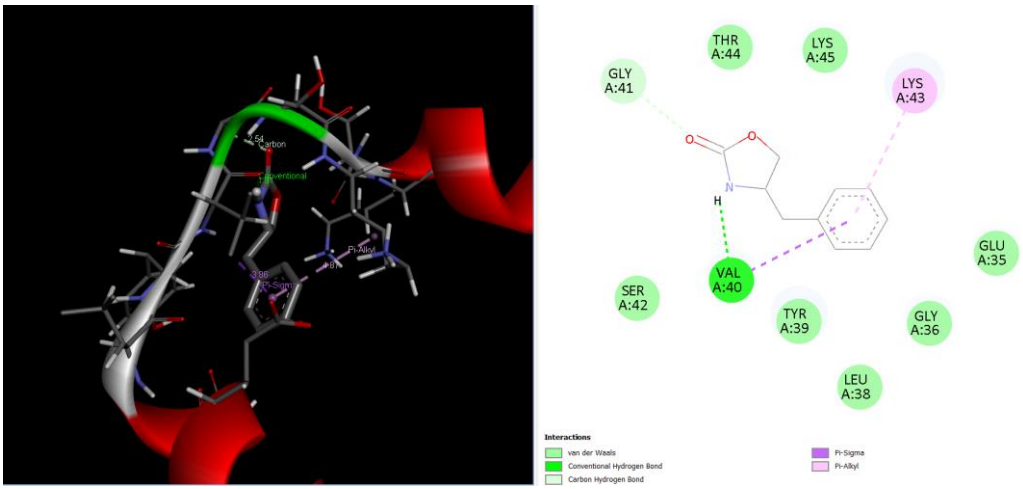

Figure 4. Molecular docking interaction of 4-Benzyl-1,3-oxazolidin-2-one with α-synuclein (PDB ID: 1XQ8). The ligand shows stable binding within the α-synuclein interaction pocket, reflected by a docking score of -5.1 kcal/mol (Table 1). The interaction pattern reveals hydrogen-bonding and hydrophobic contacts that may influence protein aggregation dynamics, suggesting a potential modulatory role in pathways associated with neurodegeneration.

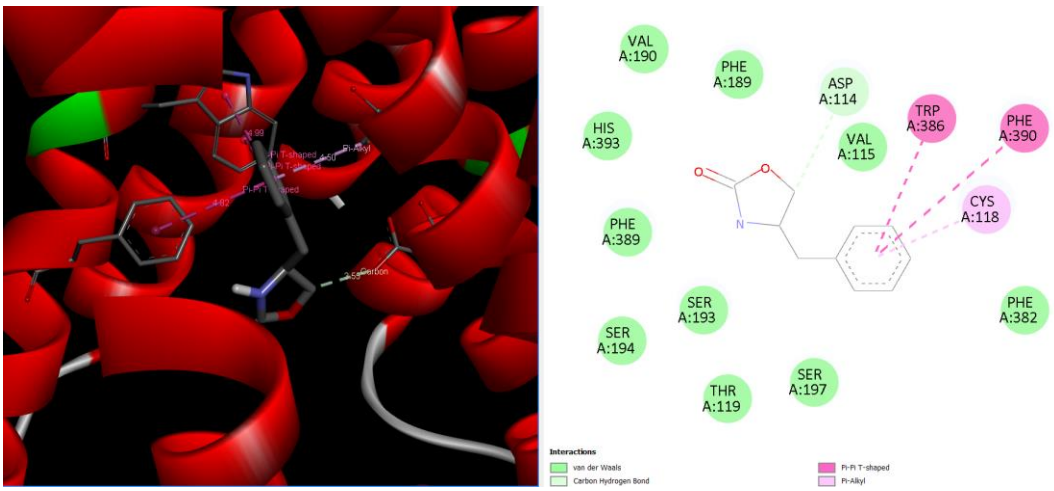

Figure 5. Molecular docking interaction of 4-Benzyl-1,3-oxazolidin-2-one with dopamine receptor complex (PDB ID: 6CM4). Showing the strongest binding affinity (-7.6 kcal/mol), the ligand forms multiple stabilizing interactions within the dopamine-receptor interface. This high-affinity binding suggests possible disruption of dopamine-mediated immunomodulatory signaling, indicating strong therapeutic potential.

Table 2. Molecular interaction profile of 4-Benzyl-1,3-oxazolidin-2-one with selected PD-related protein targets.

Sr. no	Protein	Interaction type	Amino acid residue	Bond distance
1.	α-synuclein	Conventional H-bonding	VAL40	1.91
		Carbon-Hydrogen bond	GLY41	2.54
		Pi-alkyl	GLY41	4.87
		Pi-Sigma	VAL40	3.86
2.	Dopamine receptor 2	Carbon-Hydrogen bond	ASP114	3.55
		Pi-Pi-T-Shaped	PHE39 TRP386	4.82 4.99
		Pi-Alkyl	CYS118	4.50
3.	NF-κB	Conventional H-bonding	LEU167	2.68
		Pi-Alkyl	ARG228	4.44
4.	TNF-α	Conventional H-bonding	PRO100 GLU116 SER99	2.38 2.58 2.76
		Amide-Pi-Stacked	PRO100	3.89

Table 3. Re-validation RMSD scores of docked complexes.

Sr. no	Protein name	PDB ID	RMSD
1.	α-synuclein	1XQ8	0.07 Å
2.	Dopamine receptor 2	6CM4	1.21 Å
3.	NF-κB	1NFK	1.31 Å
4.	TNF-α	1TNF	0.01 Å

3.4. Normal model analysis.

3.4.1. B-factor/mobility.

B-factors, or temperature factors, reflect atomic mobility in protein crystal structures and are widely used to identify flexible or dynamic regions. Higher B-factor values correspond to increased structural motion and disorder, whereas lower values indicate rigid, stable domains essential for maintaining protein integrity [25]. The relationship between B-factors and dynamic behavior has been reinforced by studies showing strong correlations with RMSF values [26]. Such integrated analyses help clarify how ligand binding alters local flexibility and stabilizes functionally important regions [25, 26]. Furthermore, combining crystallographic mobility patterns with simulation-based dynamics improves the prediction of functional motions and the identification of aggregation-prone regions, such as the α-synuclein NAC domain, which is relevant to PD [27]. Main-chain deformability is a measure of a

molecule's ability to deform at each of its residues. The locations of the chain's hinges can be inferred from high-deformability regions, as shown in Figures 6 and 7.

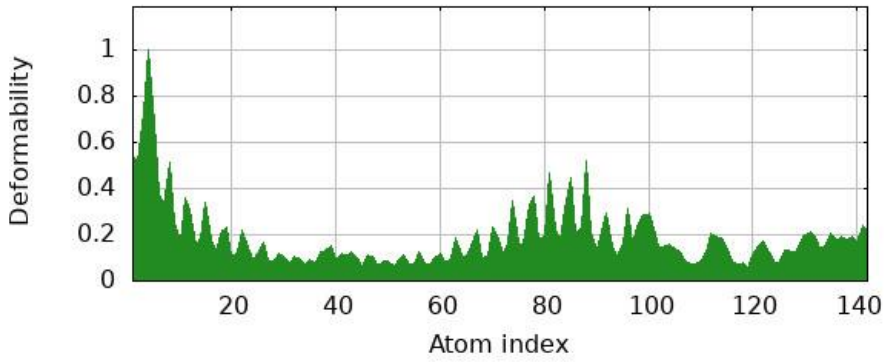

Figure 6. Deformability index of 4-Benzyl-1,3-oxazolidin-2-one with α-synuclein.

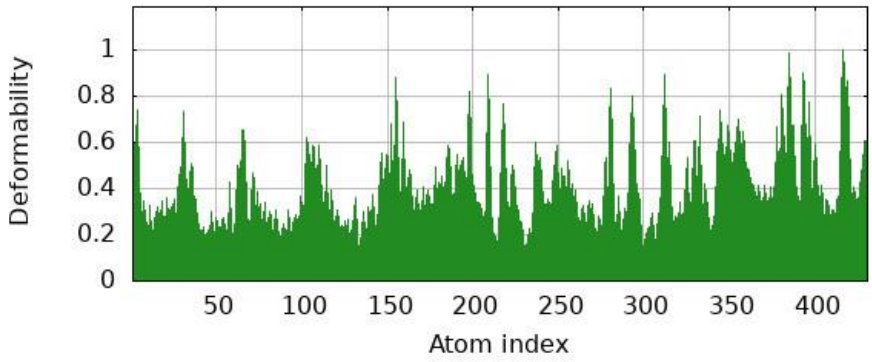

Figure 7. Deformability index of 4-Benzyl-1,3-oxazolidin-2-one with dopamine. The experimental B-factor is taken from the corresponding PDB field, and the calculated B-factor from NMA is obtained by multiplying the NMA mobility by (8pi^2). Be aware that many PDB files of averaged NMR models contain no B-factors (the B-factor column actually reports an averaged RMS).

The deformability profile of 4-Benzyl-1,3-oxazolidin-2-one bound to α-synuclein shows a characteristic pattern dominated by the intrinsically disordered nature of the α-synuclein chain. The complex displays high flexibility at the N-terminus, reduced mobility in the central NAC region, and renewed fluctuations toward the C-terminus, indicating that ligand binding does not eliminate the protein's inherent dynamic disorder. In contrast, the deformability behavior of 4-Benzyl-1,3-oxazolidin-2-one within the dopamine-associated system (protein-dopamine environment) exhibits a very different mobility distribution, with more than 400 atom indices showing periodic, localized peaks typical of a folded and compact protein structure. In this context, the ligand resides in a more structurally constrained environment where mobility arises from specific flexible loop regions rather than global chain disorder. Overall, 4-Benzyl-1,3-oxazolidin-2-one bound to α-synuclein reflects the broad, diffuse fluctuations of an intrinsically disordered protein, whereas its interaction within the dopamine-related protein system corresponds to a more rigid, structured scaffold with localized deformability. This contrast emphasizes that the same ligand experiences vastly different dynamic environments depending on whether it is associated with a disordered target such as α-synuclein or a more ordered protein system involved in dopamine binding. The deformability results indicate that 4-Benzyl-1,3-oxazolidin-2-one does not stabilize α-synuclein, as the protein remains highly flexible and intrinsically disordered even after binding. In contrast, the molecule shows more stable and structured interactions within the dopamine-related protein

environment, suggesting greater compatibility with dopaminergic systems than with α-synuclein.

3.4.2. Mobility/B-factors.

The B-factor comparison shows that 4-Benzyl-1,3-oxazolidin-2-one bound to α-synuclein produces a mobility profile dominated by the protein's intrinsic disorder, with high NMA-predicted B-factors throughout the N-terminal region and fluctuating mobility toward the C-terminus. The experimental PDB B-factor remains low, confirming that α-synuclein stays flexible even after ligand binding. In contrast, the B-factor pattern for 4-Benzyl-1,3-oxazolidin-2-one bound within the dopamine-related protein environment exhibits a much more structured and periodic mobility distribution, with NMA peaks occurring at defined segments corresponding to loop and turn regions of a folded protein, as shown in Figures 8 and 9.

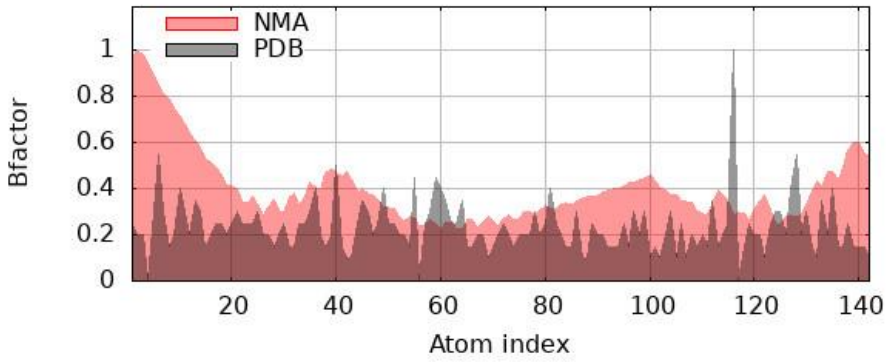

Figure 8. Mobility/B-factors of 4-Benzyl-1,3-oxazolidin-2-one with α-synuclein.

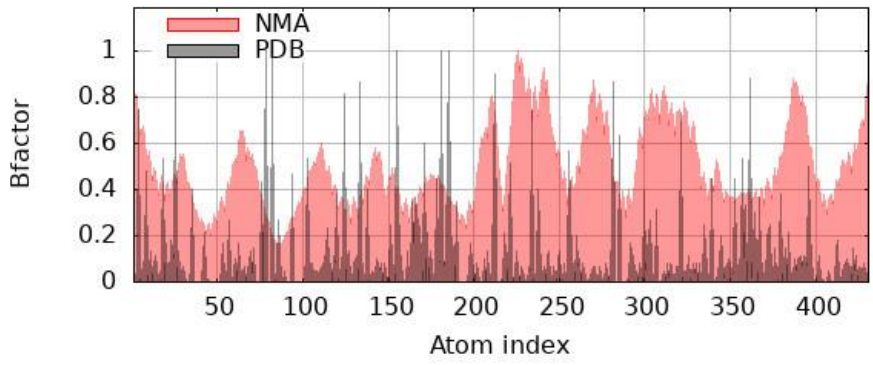

Figure 9. Deformability index of 4-Benzyl-1,3-oxazolidin-2-one with dopamine.

Here, experimental B-factors closely follow the NMA prediction, indicating that the ligand fits into a more rigid and well-organized binding environment. Overall, the ligand maintains α-synuclein's disordered flexibility but shows greater structural compatibility and more stable interactions within the dopamine-associated protein system.

3.5. Eigenvalues.

Eigenvalues derived from principal component analysis (PCA) represent the magnitude of collective motions within a protein system, with larger eigenvalues indicating dominant global fluctuations [28]. These values help distinguish essential, biologically meaningful motions from random thermal noise. Higher eigenvalues typically correspond to large-scale domain movements, while lower ones reflect minor local oscillations. In dynamics studies,

analyzing eigenvalues allows researchers to understand how ligand binding alters protein dynamics and stability. Such assessments are particularly valuable for identifying functional motions and conformational changes relevant to disease mechanisms [29]. The lower the eigenvalue, the easier the deformation, as shown in fig. 10 and 11. Comparative eigenvalue distribution plots for 4-Benzyl-1,3-oxazolidin-2-one docked with two key neurological targets. The first plot shows its interaction with α-synuclein, where the normalized eigenvalue (1) is 3.97×10^{-7}, indicating a highly flexible and weakly constrained initial mode. The second plot represents its interaction with dopamine, exhibiting a comparatively higher eigenvalue (1) of 1.59×10^{-5}, reflecting relatively greater structural rigidity. Together, these profiles illustrate differences in molecular stability and dynamic behavior across the two target-binding scenarios.

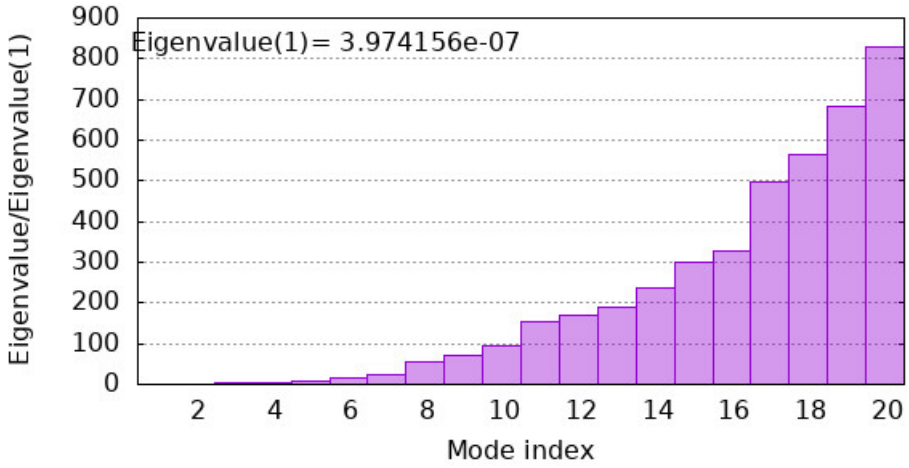

Figure 10. Eigenvalue (1) of 4-Benzyl-1,3-oxazolidin-2-one with α-synuclein.

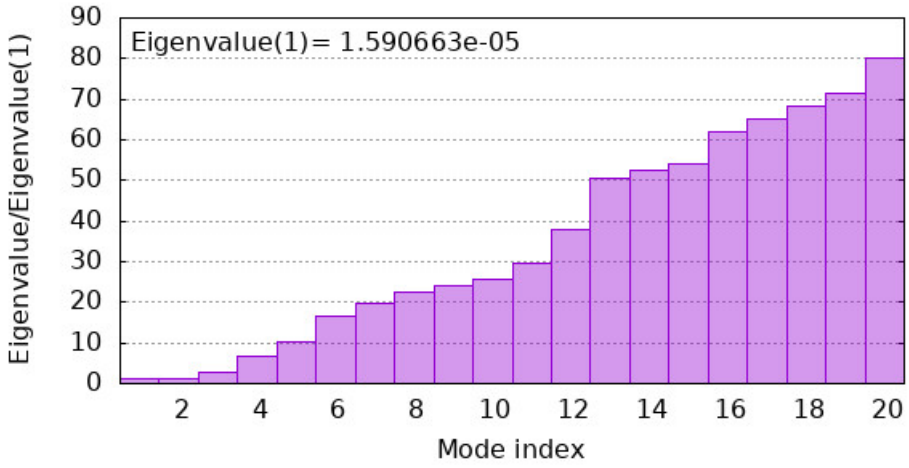

Figure 11. Eigenvalue (1) of 4-Benzyl-1,3-oxazolidin-2-one with dopamine.

3.6. Variance.

Variance percentage in PCA represents the proportion of total atomic motion explained by each principal component, helping identify which modes contribute most to overall protein dynamics [28]. Higher variance % indicates dominant collective motions, whereas lower percentages correspond to minor local fluctuations. In MD, the first few components typically capture the majority of motion, reflecting essential conformational changes. Evaluating variance % allows researchers to determine how ligand binding influences structural flexibility and the distribution of dynamic modes. This analysis also helps differentiate biologically

relevant motions from background noise, improving the interpretation of functional protein behavior [29]. The variance associated with each normal mode is inversely related to the eigenvalue. Colored bars show the individual (red) and cumulative (green) variances as shown in Figures 12 and 13. The interaction of 4-Benzyl-1,3-oxazolidin-2-one with α-synuclein and dopamine reveals distinct mechanistic implications relevant to neurodegenerative research. When paired with α-synuclein, 4-Benzyl-1,3-oxazolidin-2-one may act as a conformational modulator, potentially interfering with the protein's aggregation pathway. The 4-Benzyl-1,3-oxazolidin-2-one-α-synuclein complex (Figure 1) shows slightly higher variance contribution in the first mode (~40%) compared to the dopamine complex (~35%). However, the dopamine complex exhibits marginally faster convergence of cumulative variance, implying slightly more distributed motion across early modes and relatively improved dynamic stability compared to the α-synuclein complex. Together, these dual profiles position 4-Benzyl-1,3-oxazolidin-2-one as a candidate for multi-target neuroprotective strategies, warranting further investigation through docking, aggregation assays, and neurotransmitter quantification models.

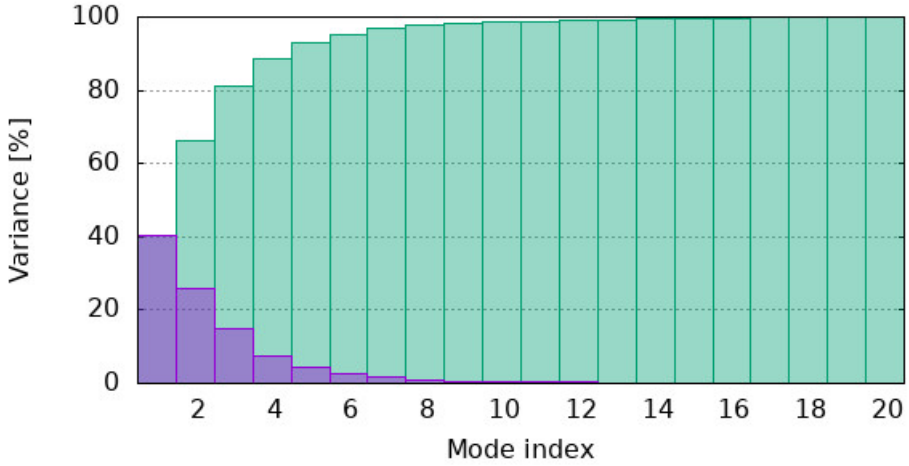

Figure 12. Variance (1) of 4-Benzyl-1,3-oxazolidin-2-one with α-synuclein.

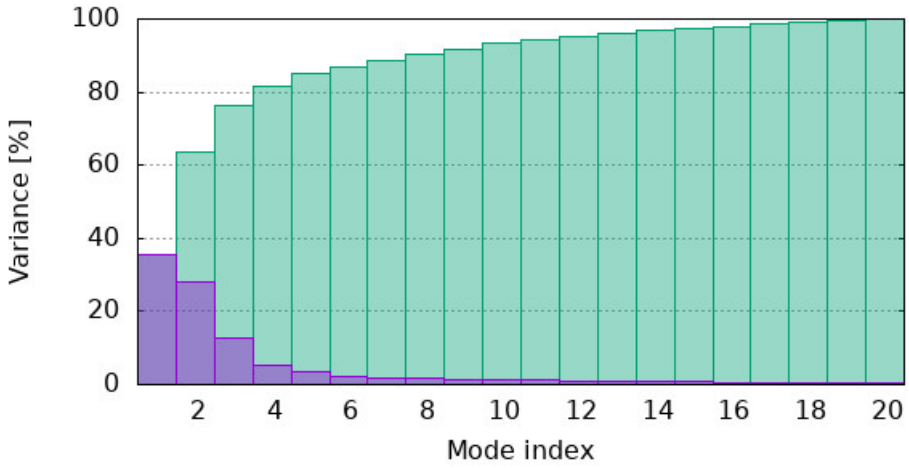

Figure 13. Variance (1) of 4-Benzyl-1,3-oxazolidin-2-one with dopamine.

3.7. Covariance map.

A covariance map illustrates the correlated and anti-correlated motions between residue pairs, revealing how different regions of a protein move relative to one another [28]. Positive covariance indicates coordinated motion in the same direction, while negative covariance reflects opposing movements that often contribute to functional dynamics. Covariance maps,

therefore, provide a powerful tool for visualizing global motion patterns and understanding the conformational mechanisms underlying disease-related proteins, as shown in Figures 14 and 15 [29]. The covariance matrix indicates coupling between pairs of residues, i.e., whether they experience correlated (red), uncorrelated (white), or anti-correlated (blue) motions. The dynamic cross-correlation matrix $C_{ij} = \frac{\langle \Delta r_i \cdot \Delta r_j \rangle}{\sqrt{\langle \|\Delta r_i\|^2 \rangle \langle \|\Delta r_j\|^2 \rangle}}$ ($-1 \leq C_{ij} \leq 1$) indicates stronger diagonal dominance in the α-synuclein complex ($N_\alpha \approx 130$), reflected by a higher local correlation ratio Λ_α, suggesting predominantly short-range cooperative motions. In contrast, the dopamine complex ($N_D \approx 420$) exhibits a higher mean absolute correlation magnitude $M_D = \frac{1}{N_D^2} \sum_{i,j} | C_{ij} |$ and greater anti-correlation density $A_D = \frac{\#(C_{ij}<0)}{N_D^2}$ relative to M_α and A_α, indicating enhanced long-range coupling. Overall, the α-synuclein complex demonstrates compact, locally coordinated dynamics, whereas the dopamine complex displays broader inter-domain communication and greater conformational adaptability.

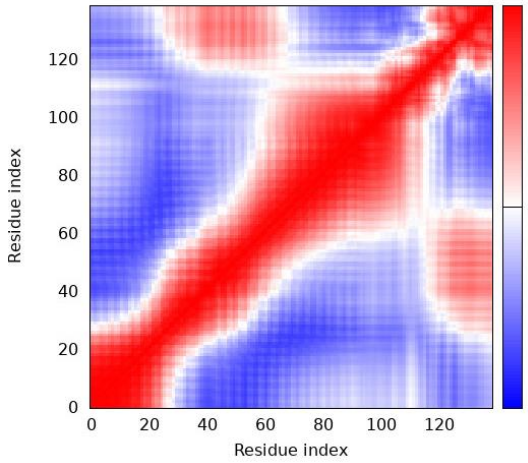

Figure 14. Residue Index of 4-Benzyl-1,3-oxazolidin-2-one with α-synuclein.

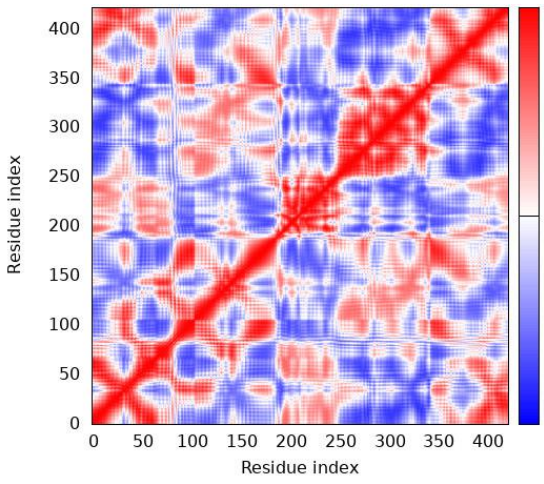

Figure 15. Residue Index of 4-Benzyl-1,3-oxazolidin-2-one with dopamine. The correlation matrix is computed using the Cα Cartesian coordinates and Equation 2.

3.8. Elastic network.

The elastic network model (ENM) defines which pairs of atoms are connected by springs. Each dot in the graph represents one spring between the corresponding pair of atoms, as shown in Figures 16 and 17. Dots are colored by stiffness; darker grays indicate stiffer springs, and vice versa.

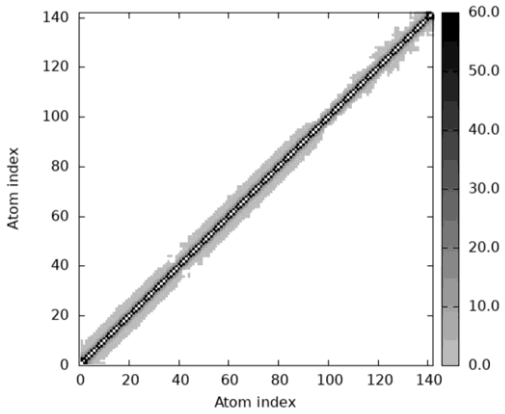

Figure 16. Atom index of 4-Benzyl-1,3-oxazolidin-2-one with α-synuclein.

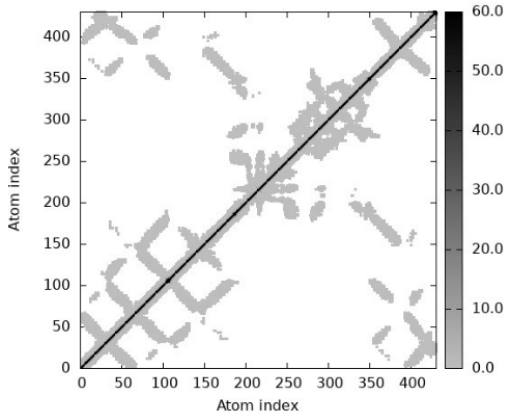

Figure 17. Atom index of 4-Benzyl-1,3-oxazolidin-2-one with dopamine.

The elastic network model (ENM) represents interatomic interactions through harmonic springs, with total elastic potential energy defined as $E = \frac{1}{2}\sum_{i,j} k_{ij}\,(r_{ij} - r_{ij}^0)^2$ where k_{ij}denotes the spring stiffness between atom pairs. In the α-synuclein complex (Fig. 16; $N_\alpha = 140$), spring connections are predominantly concentrated within the 0-140 atom index range, with comparatively higher local stiffness values ($k_{ij}^\alpha \approx$ 0.8-1.0), indicating dense mechanical coupling and compact structural rigidity. In contrast, the dopamine complex (Fig. 17; $N_D = 450$) exhibits a broader connectivity matrix spanning the 0-450 atom index range, with more distributed stiffness values ($k_{ij}^D \approx$ 0.4-0.9), reflecting extended long-range elastic interactions. Therefore, while the α-synuclein complex demonstrates higher localized stiffness density and mechanical compactness, the dopamine complex shows greater spatial dispersion of elastic connections, consistent with increased mechanical flexibility and dynamic adaptability.

3.9. RMSF of 4-benzyl-1,3-oxazolidin-2-one.

The comparative RMSF analysis demonstrates that 4-Benzyl-1,3-oxazolidin-2-one interacts very differently with α-synuclein and dopamine, highlighting its dual potential relevance in PD, as shown in Figures 18 and 19.

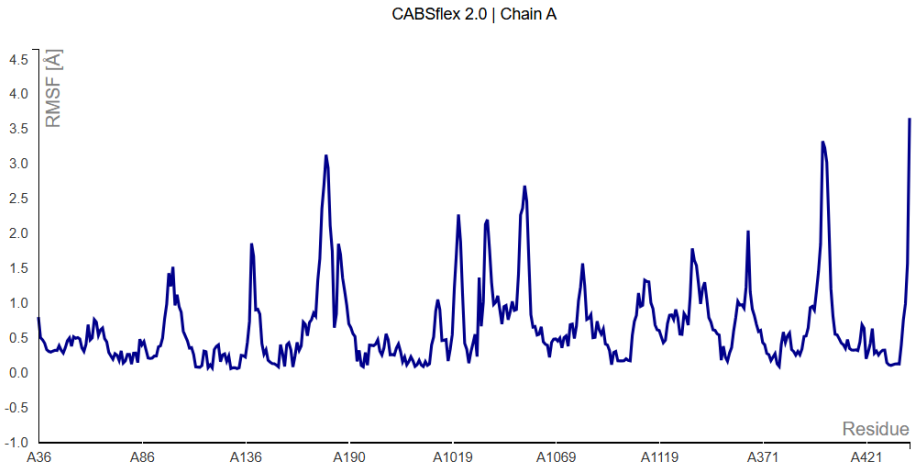

Figure 18. Graphical representation of the RMSF of 4-Benzyl-1,3-oxazolidin-2-one with dopamine.

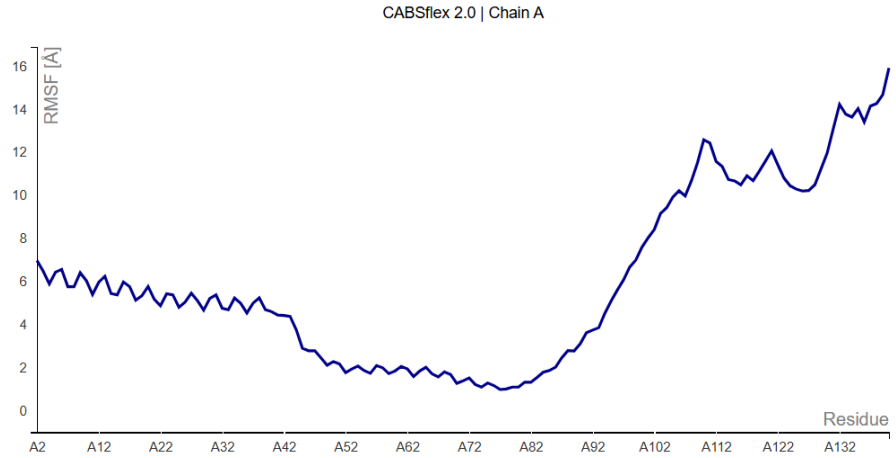

Figure 19. Graphical representation of the RMSF of 4-Benzyl-1,3-oxazolidin-2-one with α-synuclein.

The compound significantly stabilizes the central NAC region of α-synuclein-an intrinsically disordered and aggregation-prone domain, suggesting a possible disease-modifying effect by reducing structural flexibility and thereby limiting fibril formation. In contrast, its interaction with dopamine shows uniformly low RMSF values, indicating a highly stable and compact binding environment that may help preserve dopaminergic function or receptor interaction, contributing to symptomatic improvement and 19. Together, these findings suggest that 4-Benzyl-1,3-oxazolidin-2-one could exert both anti-aggregation and dopamine-supportive effects, making it a promising candidate for further investigation in PD therapy.

4. Conclusion

The current work represents a comprehensive computational assessment of 4-Benzyl-1,3-oxazolidin-2-one to investigate its potential interactions with molecular targets involved in PD. ADMET profiling in silico indicated good drug-likeness characteristics, estimated BBB permeability, and an overall positive pharmacokinetic signature. Prediction models of toxicity showed low theoretical risks of hepatotoxicity and cardiotoxicity, but the results are just predictions and need testing. Molecular docking studies revealed energetically favorable interactions with selected PD-associated targets, including NF-κB, TNF-α, the dopamine receptor complex, and synuclein. The interactions identified may moderate the neuroinflammatory signaling and protein aggregation pathways, but no functional biological

impacts can be determined solely from docking scores. Normal mode analysis also suggested that the chosen ligand-protein complexes were structurally stable, with minimal changes in conformation and maintained interaction profiles within the predicted binding regions. All these computational results indicate that 4-Benzyl-1,3-oxazolidin-2-one is structurally feasible as a multi-target binding scaffold. The findings must, however, be viewed as initial in-silico facts but not a validation of therapeutic effectiveness. The validation of biological activity, the evaluation of pharmacodynamic relevance, and the safety profile must be assessed through experimental in vitro and in vivo studies. This paper presents a mechanistic computational framework for evaluating oxazolidinone derivatives in future PD research.

Author Contributions

Conceptualization, L.S. and D.D.; methodology, L.S.; software, A.S.; validation, A.S., L.S. and D.D.; formal analysis, A.S.; investigation, L.S.; data curation, D.D.; writing—original draft preparation, A.S.; writing—review and editing, D.D.; visualization, D.D.; supervision, L.S. All authors have read and agreed to the published version of the manuscript.

Institutional Review Board Statement

Not applicable.

Informed Consent Statement

Not applicable.

Data Availability Statement

Data supporting the findings of this study are available upon reasonable request from the corresponding author.

Funding

The authors declare that no funds, grants, or other support were received during the preparation of this manuscript.

Acknowledgments

The authors are thankful to UIPS and Chandigarh University for their support and encouragement in this work.

Conflicts of Interest

The authors declare no conflict of interest.

Abbreviations

The following abbreviations are used in this manuscript:

Abbreviation	Definition
ADMET	Absorption, Distribution, Metabolism, Excretion, and Toxicity
AMES	Ames Mutagenicity Test
BBB	Blood-Brain Barrier
CADD	Computer-Aided Drug Design

Abbreviation	Definition
CNS	Central Nervous System
CYP	Cytochrome P450 Enzyme System
DILI	Drug-Induced Liver Injury
ENM	Elastic Network Model
GI	Gastrointestinal
HIA	Human Intestinal Absorption
IL-1β	Interleukin-1 Beta
IL-6	Interleukin-6
LogP	Partition Coefficient (lipophilicity)
MAO-B	Monoamine Oxidase-B
MD	Molecular Dynamics
MW	Molecular Weight
NAC	Non-Amyloid-β Component Region of α-synuclein
NMA	Normal Mode Analysis
NF-κB	Nuclear Factor Kappa-Light-Chain-Enhancer of Activated B Cells
PCA	Principal Component Analysis
PD	Parkinson's disease
PDB	Protein Data Bank
PkCSM	Pharmacokinetics Computational Models
P-gp / PGP	P-glycoprotein
Rg	Radius of Gyration
RMS	Root Mean Square
RMSF	Root Mean Square Fluctuation
ROS	Reactive Oxygen Species
TPSA	Topological Polar Surface Area
TNF-α	Tumor Necrosis Factor-Alpha
VDss	Volume of Distribution at Steady State

References

1. Aksoy, A.; Usta, D.D.; Yar Saglam, A.S. Current Treatments for Parkinson's Disease. *J. Biomed. Res. Environ. Sci.* **2024**, *5*, 1602-16150, https://doi.org/10.37871/jbres2047.
2. Feigin, V.L.; Vos, T.; Nichols, E.; Owolabi, M.O.; Carroll, W.M.; Dichgans, M.; Deuschl, G.; Parmar, P.; Brainin, M.; Murray, C. The global burden of neurological disorders: translating evidence into policy. *Lancet Neurol.* **2020**, *19*, 255-265, https://doi.org/10.1016/s1474-4422(19)30411-9.
3. Mitchell, C.L.; Kurouski, D. Novel strategies in Parkinson's disease treatment: a review. *Front. Mol. Neurosci.* **2024**, *17*, 1431079, https://doi.org/10.3389/fnmol.2024.1431079.
4. Merghany, R.M.; El-Sawi, S.A.; Naser, A.F.A.; Ezzat, S.M.; Moustafa, S.F.A.; Meselhy, M.R. A comprehensive review of natural compounds and their structure–activity relationship in Parkinson's disease: exploring potential mechanisms. *Naunyn Schmiedebergs Arch. Pharmacol.* **2025**, *398*, 2229-2258, https://doi.org/10.1007/s00210-024-03462-4.
5. Balestri, W.; Sharma, R.; da Silva, V.A.; Bobotis, B.C.; Curle, A.J.; Kothakota, V.; Kalantarnia, F.; Hangad, M.V.; Hoorfar, M.; Jones, J.L.; Tremblay, M.-È.; El-Jawhari, J.J.; Willerth, S.M.; Reinwald, Y. Modeling the neuroimmune system in Alzheimer's and Parkinson's diseases. *J. Neuroinflammation* **2024**, *21*, 32, https://doi.org/10.1186/s12974-024-03024-8.
6. Haider, A.; Elghazawy, N.H.; Dawoud, A.; Gebhard, C.; Wichmann, T.; Sippl, W.; Hoener, M.; Arenas, E.; Liang, S.H. Translational molecular imaging and drug development in Parkinson's disease. *Mol. Neurodegeneration* **2023**, *18*, 11, https://doi.org/10.1186/s13024-023-00600-z.
7. Majbour, N. K.; Vaikath, N. N.; Van Dijk, K. D.; Ardah, M. T.; Varghese, S.; Vesterager, L. B.; El-Agnaf, O. M. A. Seeded aggregation assays for α-synuclein as biomarkers in Parkinson's disease. *Mov. Disord.* **2022**, *37*, https://doi.org/10.1212/WNL.0000000000201199.
8. Levin, J.; Wrasidlo, W.; Price, E.; Winter, F.; Hall, M.; Maass, F.; Schmitt, I.; Haass, C. Phase 1 clinical evaluation of anle138b targeting α-synuclein aggregation. *Neurology* 2022, *98*, https://doi.org/10.1016/j.ebiom.2022.104021.
9. Singh, A.; Singh, L.; Dalal, D. Mechanistic insights into the therapeutic potential of apigenin in Parkinson's disease: An in silico docking and ADMET study. *Curr. Behav. Neurosci. Rep.* **2026**, *13*, 1, https://doi.org/10.1007/s40473-026-00319-3.

10. Żulińska, S.; Strosznajder, A.K.; Strosznajder, J.B. Current View on PPAR-α and Its Relation to Neurosteroids in Alzheimer's Disease and Other Neuropsychiatric Disorders: Promising Targets in a Therapeutic Strategy. *Int. J. Mol. Sci.* **2024**, *25*, 7106, https://doi.org/10.3390/ijms25137106.
11. Pizcueta, P.; Vergara, C.; Emanuele, M.; Vilalta, A.; Rodríguez-Pascau, L.; Martinell, M. Development of PPARγ Agonists for the Treatment of Neuroinflammatory and Neurodegenerative Diseases: Leriglitazone as a Promising Candidate. *Int. J. Mol. Sci.* **2023**, *24*, 3201, https://doi.org/10.3390/ijms24043201.
12. Titus, C.; Hoque, M.T.; Bendayan, R. PPAR agonists for the treatment of neuroinflammatory diseases. *Trends Pharmacol. Sci.* **2024**, *45*, 9-23, https://doi.org/10.1016/j.tips.2023.11.004.
13. Wolff, A.; Schumacher, N.U.; Pürner, D.; Machetanz, G.; Demleitner, A.F.; Feneberg, E.; Hagemeier, M.; Lingor, P. Parkinson's disease therapy: what lies ahead? *J. Neural Transm.* **2023**, *130*, 793-820, https://doi.org/10.1007/s00702-023-02641-6.
14. Feng, A.; Zeng, Q.; Wang, J.; Li, H.; Fang, X.; Geng, Y.; Pan, W.; Li, G.; Dong, J. Synthesis of novel pyrazole derivatives and neuroprotective effect investigation. *J Enzyme Inhib Med Chem*. **2025** *40*, 2583820, https://doi.org/10.1080/14756366.2025.2583820.
15. Pandit, N.; Singla, R.K.; Shrivastava, B. Current Updates on Oxazolidinone and Its Significance. *Int. J. Med. Chem.* **2012**, *2012*, 159285, https://doi.org/10.1155/2012/159285.
16. Yuan, L.; Sheng, R.; Guan, M.; Wang, Y.; Chen, S. Biologically active 2-oxazolidinone derivatives beyond antibacterial activities. *Curr. Med. Chem*. **2023**, *30*, 2672-2689, https://doi.org/10.2174/0929867329666220823113415.
17. Durrant, J. D.; McCammon, J. A. Molecular dynamics simulations and drug discovery. *BMC Biology* **2011**, *9*, 71, https://doi.org/10.1186/1741-7007-9-71.
18. Daina, A.; Michielin, O.; Zoete, V. SwissADME: a free web tool to evaluate pharmacokinetics, drug-likeness and medicinal chemistry friendliness of small molecules. *Sci. Rep.* **2017**, *7*, 42717, https://doi.org/10.1038/srep42717.
19. Yang, H.; Lou, C.; Sun, L.; Li, J.; Cai, Y.; Wang, Z.; Li, W.; Liu, G.; Tang, Y. admetSAR 2.0: web-service for prediction and optimization of chemical ADMET properties. *Bioinformatics* **2019**, *35*, 1067-1069, https://doi.org/10.1093/bioinformatics/bty707.
20. Meng, X.Y.; Zhang, H.X.; Mezei, M.; Cui, M. Molecular docking: a powerful approach for structure-based drug discovery. *Curr. Comput.-Aided Drug Des*. **2011**, *7*(2), 146-157, https://doi.org/10.2174/157340911795677602.
21. Alikhani, R.; Ebadi, A.; Karami, P.; Shahbipour, S.; Razzaghi-Asl, N. Response surface study on molecular docking simulations of citalopram and donepezil as potent CNS drugs. *Iran. J. Pharm. Res.* **2021**, *20*, 560–576, https://doi.org/10.22037/ijpr.2020.113644.14409.
22. Yousaf, A.; Singh, A.; Dalal, D. Fisetin as a neuroprotective agent: Docking-based modulation of dopaminergic and inflammatory pathways in Parkinson's disease. *Neurophysiology* **2024**, *56*, 18-27, https://doi.org/10.1007/s11062-025-09981-x.
23. López-Blanco, J.R.; Aliaga, J.I.; Quintana-Ortí, E.S.; Chacón, P. iMODS: internal coordinates normal mode analysis server. *Nucleic Acids Res.* **2014**, *42*, W271-W276, https://doi.org/10.1093/nar/gku339.
24. Kuriata, A.; Gierut, A.M.; Oleniecki, T.; Ciemny, Maciej P.; Kolinski, A.; Kurcinski, M.; Kmiecik, S. CABS-flex 2.0: a web server for fast simulations of flexibility of protein structures. *Nucleic Acids Res.* **2018**, *46*, W338-W343, https://doi.org/10.1093/nar/gky356.
25. Carugo, O.; Argos, P. Correlation between side chain mobility and conformation in protein structures. *Protein Eng*. **1997**, *10*, 777-787, https://doi.org/10.1093/protein/10.7.777.
26. Pandey, A.; Liu, E.; Graham, J.; Chen, W.; Keten, S. B-factor prediction in proteins using a sequence-based deep learning model. *Patterns* **2023**, *4*(9), 100805, https://doi.org/10.1016/j.patter.2023.100805.
27. Uversky, V.N. Intrinsically disordered proteins and their (disordered) proteomes in neurodegenerative disorders. *Front. Aging Neurosci.* **2015**, *7*, 18, https://doi.org/10.3389/fnagi.2015.00018.
28. Amadei, A.; Linssen, A.B.M.; Berendsen, H.J.C. Essential dynamics of proteins. *Protein Struct. Funct. Bioinform.* **1993**, *17*, 412-425, https://doi.org/10.1002/prot.340170408.
29. David, C.C.; Jacobs, D.J. Principal component analysis: a method for determining the essential dynamics of proteins. *Methods Mol. Biol.* **2014**, *1084*, 193-226, https://doi.org/10.1007/978-1-62703-658-0_11.

Publisher's Note & Disclaimer